Crystal Structure and Morphology of Poly(11-undecalactone) Solution-Grown Single Crystals

Eunju Kim,[†,‡] Hiroshi Uyama,[§] Yoshiharu Doi,[‡,⊥] Chang-Sik Ha,[†] and Tadahisa Iwata*[,‡]

Department of Polymer Science and Engineering, Pusan National University, Pusan 609-735, Korea; Polymer Chemistry Laboratory, RIKEN Institute, 2-1 Hirosawa, Wako-shi, Saitama 351-0198, Japan; Graduate School of Engineering, Osaka University, 2-1 Yamadagaoka, Suita, Osaka 565-0871, Japan; and Department of Innovative and Engineered Materials, Tokyo Institute of Technology, 4259 Nagatsuta, Midori-ku, Yokohama 226-8502, Japan

Received April 13, 2004; Revised Manuscript Received June 15, 2004

ABSTRACT: Solution-grown lamellar single crystals of poly(11-undecalactone) (PUDL) have been prepared in 1-hexanol. The lozenge and hexagonal-shaped single crystals were grown simultaneously, and these crystals gave well-resolved electron diffraction diagrams from which the orthogonal reciprocal lattice with the parameters $a^* = 1.346$ nm^{-1}, $b^* = 2.004$ nm^{-1}, and $\gamma^* = 90°$ could be determined. The growth faces of both crystals were considered as mainly {110}, and the average chain-folding direction was parallel to these growth planes, suggesting that the hexagonal crystal has pseudohexagonal symmetry but actual orthogonal packing of the PUDL molecules. The diffraction analysis combined with X-ray and electron diffraction diagrams indicated that PUDL crystallized in the orthorhombic system which had the lattice parameters of $a = 0.743 \pm 0.001$ nm, $b = 0.499 \pm 0.001$ nm, and c(chain axis) $= 1.519 \pm 0.003$ nm. There are two chains per unit cell, which existed in an antiparallel arrangement. The fiber repeat distance is appropriate for an all-trans backbone conformation for the straight stems. Molecular packing of this structure has been studied in detail, taking into account both diffraction data and energy calculations. The setting angles, with respect to a axis, were 59° for the corner and center chains according to intensity measurements and structure factor calculations. A final model was obtained to yield $R = 0.173$ with X-ray diffraction data and $R = 0.152$ with electron diffraction data. A brief comparison is also made with related polymer structures.

Introduction

Recently, the synthesis of aliphatic polyesters by various monomer combinations through lipase catalysis has been extensively investigated.[1−4] An optically active polyester was also enantioselectively synthesized by lipase-catalyzed polycondensation of a racemic epoxide-containing activated diester with a diol monomer.[5] Lipase also induced ring-opening polymerization and copolymerization of lactones,[6−19] lactide,[14,20] and six-membered cyclic carbonate.[21−23] Until now, small-size (4-membered)[6−10] and medium-size lactones (6- and 7-membered)[11−14] as well as macrolides (12-, 13-, 16-, and 17-membered)[15−19] have been subjected to the lipase-catalyzed polymerization. Normally, macrolides show much lower reactivity and polymerizability in an anionic process than ϵ-caprolactone (ϵ-CL) due to their lower ring strain.[4] However, they were enzymatically polymerized much faster than ϵ-CL. This is probably due to a favored transition state of the macrolide to open the ring with lipase catalysis.[24]

The crystal structures of aliphatic polyester, $-(-O-(CH_2)_m-CO-)_n-$, have been aggressively studied by many research groups on the basis of X-ray diffraction of stretched films and electron diffraction of solution-grown lamellar crystals combined with energy calculation. Until now, the crystal and molecular structures of poly(β-propiolactone) (PPL, $m = 2$),[25−27] poly(4-hydroxybutyrate) (P(4HB), $m = 3$),[28−33] poly(δ-valerolactone) (PVL, $m = 4$),[34] poly(ϵ-caprolactone) (PCL, $m = 5$),[35−40] and poly(ω-pentadecalactone) (PPDL, $m = 14$)[41] have been reported.

PPL has mainly three different chain conformations and crystal structures: α- and β-forms obtained from oriented films with different conditions and γ-form originated from solution-grown lamellar crystals. The chain conformation of α-form has a 2-fold helix with a fiber repeat of 0.702 nm, thus, an advance per monomer of 0.702/2 = 0.351 nm. This latter value is 26% less than that expected for the all-trans planar structure.[25] The orthorhombic unit cell dimensions of the β-form, which is represented as an all-trans conformation, were reported as $a = 0.773$ nm, $b = 0.448$ nm, and c(chain axis) $= 0.477$ nm.[26] The γ-structure has been discovered from the solution-grown, chain-folded lathlike lamellar crystals. The chain is in an all-trans or 1-fold helix conformation, and the structure consists of a two-chain, C-faced, orthorhombic unit cell with the following parameters: $a = 0.700$ nm, $b = 0.490$ nm, and c(chain axis) $= 0.493$ nm.[27] The setting angles, with respect to the a axis, are ±51.5° for the corner and center chains.

The crystal structure of P(4HB) is an orthorhombic with space group $P2_12_12_1$ and parameters $a = 0.775$ nm, $b = 0.477$ nm, and c(chain axis) $= 1.199$ nm.[28,29,31] There are two chains per unit cell, which exist in an antiparallel arrangement. The helical conformation is characterized as a slightly distorted all-trans conformation. The setting angles, with respect to the a axis, are ±61° for the corner and center chains according to intensity measurements and structure factor calculations. The

† Pusan National University.
‡ RIKEN Institute.
§ Osaka University.
⊥ Tokyo Institute of Technology.
* To whom all correspondence should be addressed: Tel +81-48-467-9586, Fax +81-48-462-4667; e-mail tiwata@riken.jp.

10.1021/ma0492871 CCC: $27.50
Published on Web 08/21/2004

Scheme 1. Definition of Atom Types in the PUDL Used as the Basic Unit in the Computes Unit Cells

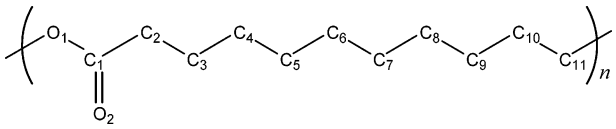

lamellar single crystals appear as lozenge-shaped crystals with screw dislocation.[33]

The diffraction signals of PVL index on an orthorhombic unit cell with the parameters $a = 0.747$ nm, $b = 0.502$ nm, and c(chain axis) $= 0.742$ nm and two antiparallel chains exist in the unit cell.[34] The c value of 0.742 nm is appropriate for an all-trans or 1-fold helical backbone conformation for the straight stems. The setting angles, with respect to the a axis, are ±58° for the corner and center chains. The chain-folded crystals terrace on top of one another as they develop into an aggregate.

Two X-ray fiber diffraction studies on PCL have been reported,[35,36] both in space groups $P2_12_12_1$ with essentially identical unit cell parameters but with appreciably different derived chain conformations and packings. Bittiger and Marchessault[35] reported that the unit cell of PCL was found to be orthorhombic with dimensions $a = 0.750$ nm, $b = 0.497$ nm, and c(chain axis) $= 1.730$ nm. This unit cell is only compatible with an extended planar chain conformation of the molecule involving two monomer residues related by a 2-fold screw axis in the chain direction. On the other hand, Chatani et al.[36] reported that the chain conformation of PCL is almost planar zigzag but evidently derives from the fully extended form (nonplanar model); i.e., the CH_2 sequences are planar, but the plane of atoms of the ester group tilts slightly to the fiber axis. They reported the unit cell parameters are $a = 0.747$ nm, $b = 0.498$ nm, and c(chain axis) $= 1.705$ nm. To resolve these conflicting results, Hu and Dorset[37] have investigated the crystal structure analysis using electron diffraction intensities of (0kl) and (hkl) obtained from epitaxially oriented crystals, combined with (hk0) data from solution-grown lancetlike crystals, and it was revealed that the nonplanar model is preferred. Furthermore, the correctness of the nonplanar conformation was eventually ascertained by direct structure analysis of 3-D electron diffraction data[38] and of the fiber X-ray data.[39] The morphology of solution-grown lamellar crystals of PCL was reported as hexagonal-shaped with growth planes of {110} and {010}.[35,40]

However, polylactones synthesized by macrolides have not been reported except 16-membered macrolide (poly(ω-pentadecalactone), PPDL, $m = 14$). Recently, the crystal structure of PPDL[41] was studied by X-ray powder diffraction pattern and fiber diagram of 200% stretched film. A pseudo-orthorhombic, monoclinic, unit cell with dimensions $a = 0.749$ nm, $b = 0.503$ nm, c(chain axis) $= 2.000$ nm, and $\alpha = 90.06°$ hosts two monomeric units belonging to polymer chains with opposite orientation, according to the $P2_1$ space-group symmetry.

We report, herein, the crystal and molecular structure of poly(11-undecalactone) (PUDL, $m = 10$, synthesized by 12-membered macrolide, Scheme 1) by X-ray diffraction and electron diffraction combined with energy calculation. Furthermore, the morphology of PUDL solution-grown single crystals was investigated by means of transmission electron microscopy (TEM) and atomic force microscopy (AFM).

Experimental Section

PUDL Samples. Poly(11-undecalactone) (PUDL) used in this study was synthesized by enzyme-catalyzed reactions in organic solvents.[15] 11-Undecanolide (UDL) was purchased from Lancaster. The monomer was purified by the addition of freshly activated type 4 molecular sieves. 2 g of monomer and 100 mg of Novozym435 as catalyst were dissolved in 4 mL of absolute-grade toluene. The polymerization was carried out at 70 °C for 24 h under an Ar atmosphere. The obtained polymer was dissolved in chloroform and precipitated from methanol to remove unreacted monomers and byproduct oligomers.

Preparation of PUDL Single Crystals. A 0.5 mg sample ($M_w = 46\,000$, $M_w/M_n = 1.80$) was dissolved into 5 mL of 1-hexanol at 80 °C and maintained at this temperature for 1 h. Slow cooling was then applied until the crystallization temperature, 52 °C, and the solution was kept there for 6 h. And then, the solution was cooled slowly until room temperature. The slow cooling was performed by cutting off the heating element of a silicone oil bath. Single crystals were recovered by centrifugation and repeatedly washed with methanol.

Transmission Electron Microscopy. Drops of crystal suspension were deposited on carbon-coated grids, allowed to dry, and then shadowed with Pt−Pd alloy. For electron diffraction purposes, the dried crystals were used directly without further treatments. These grids were observed with a JEM-2000FX II electron microscope operated at an acceleration voltage of 120 kV for electron diffraction and for the imaging of shadowed crystals. Calibration of the electron diffraction patterns was done after depositing the crystals on gold-coated grids. The observed intensities (I_{obs}) of electron reflections recorded on Fuji imaging plates were measured by using R-axis display software (Rigaku). The observed structure factor (F_{obs}) was taken as the square root of corresponding intensities.

X-ray Measurement. Oriented crystal mats suitable for X-ray diffraction were prepared by sucking the crystal suspension through a 0.1 μm PTFE filter using a water aspirator. The wide-angle X-ray diffraction patterns were obtained at room temperature, using Ni-filtered Cu Kα radiation of wavelength 0.154 18 nm, from a Rigaku RINT UltraX 18 sealed beam X-ray generator operating at 40 kV and 110 mA. The X-ray beam was directed parallel to the mat surface for the oriented mats. The X-ray diffraction patterns were recorded using a point-collimated beam and a flat-plate film holder in an evacuated camera. X-ray diffraction patterns of solvent-cast film annealed at 70 °C for 24 h of PUDL were recorded on a RINT 2500 operating at 40 kV and 110 mA with Ni-filtered Cu Kα radiation. The scan was carried out in the $\theta/2\theta$ reflection mode by the Rietveld method.[42,43] The conditions of scan are that a divergence aperture is 0.3°, receiving aperture is 0.05°, step width is 0.5°, count time is 60 s per step, and 2θ range is 2°−60°.

Atomic Force Microscopy. The lamellar thickness of single crystals of PUDL was investigated on the basis of atomic force microscopy (AFM). AFM was performed with a SPA400/SPI3800N (Seiko Instruments Inc., Japan) in a dynamic force microscope (DFM) mode. A rectangular silicon cantilever (Si-DF3, 450 μm in length, resonant frequency of ca. 14 kHz, stiffness of ca. 0.15 N/m) were applied in all experiments. All measurements were carried out in ambient condition. The resulting images were flattened and plane-fit using Seiko Instruments software.

Molecular Weight Measurement. The molecular weights of PUDL were measured by GPC at 40 °C consisting of a Shimadzu 10A GPC system and a 6A refractive index detector with joint columns of Shodex K-80M and K-802 (each 4.6 × 300 mm). Chloroform was used as an eluent at a flow rate of 0.8 mL/min. The number- and weight-average molecular weights (M_n and M_w) were calculated by using a Shimadzu

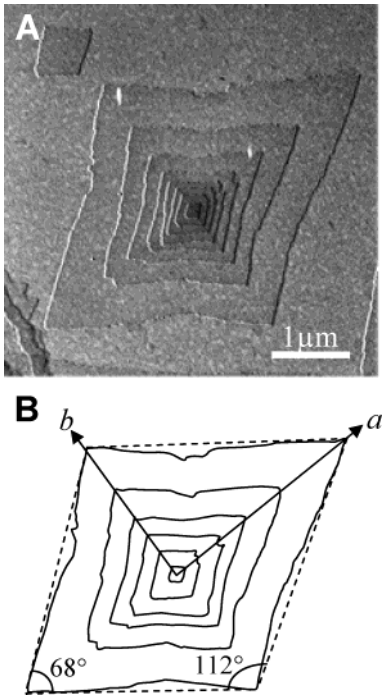

Figure 1. (A) Transmission electron micrograph after shadowing with Pt−Pd alloy of PUDL lozenge-shaped lamellar single crystals. (B) A schematic display of lozenge-shaped single crystals.

Chromatopac C-R7A plus equipped with a GPC program. Molecular weight was obtained with polystyrene standards of low polydispersities.

Model Building and Analyses of Structure. The software package Cerius^2, version 4.2 (Accelrys, Inc.), was used in the structural modeling and diffraction simulations. The basic strategy was to determine the molecular conformation of the PUDL chain and the molecular packing arrangement within the unit cell. After the initial model building stage, a combination of energy minimization and simulations of diffraction patterns was used. This ensured that the model was stereochemically sound and that the simulated diffraction patterns were in good agreement with experimental data. In the computer-simulated X-ray diffraction patterns, the degree of arcing and intensity were chosen to match the experimental electron and X-ray diffraction patterns as closely as possible.

Results and Discussion

Lamellar Single Crystals. Two kinds of poly(11-undecalactone) (PUDL) single-crystal morphologies were obtained simultaneously from a dilute solution of 1-hexanol, as shown in Figures 1 and 2. The single crystals in Figure 1 appear as lozenge-shaped multilayer single crystals, and the ratio between the two diagonal axes of the lozenge-shaped crystals was about 4:3. The crystallographic *a* and *b* axes were determined by the triple exposure of selected-area electron diffraction and the normal and selected-area images. In general, the crystals taper to a point, often with a half-angle of approximately 34° relative to the long axis of the crystals. There seems to be a correlation between this value and an angle of 34° between the crystallographic diagonal {110} planes and the *a* axis on the unit cell. This crystal morphology has been reported for single crystals of polyethylene[44] and *n*-hexatriacontane (*n*-$C_{36}H_{74}$).[45] The growth faces of the lamellar are not a straight line. This indicates that the apexes of the lozenge-shaped crystal grow outward at a more rapid rate than the edges between two apexes. This phenomenon was reported in spiral growths on a polyoxymethylene crystal.[46] A line approximately normal to the line connecting two adjacent apexes is referred to as a slow growth line. Furthermore, many lamellar crystals have one centrally located additional lamella on the basal lamella. This observation has been reported for single crystals of polyethylene,[44] poly(3,3-bis(chloromethyl-oxacyclobutane),[47] poly[(*R*)-3-hydroxyvalerate] (P(3HV)),[48] and so on. In the case of PUDL crystals, since a small bump can be also observed on the crystal surface as the primary nucleus, the basal lamella and the additional lamellae seem to be grown from the same primary nucleus.

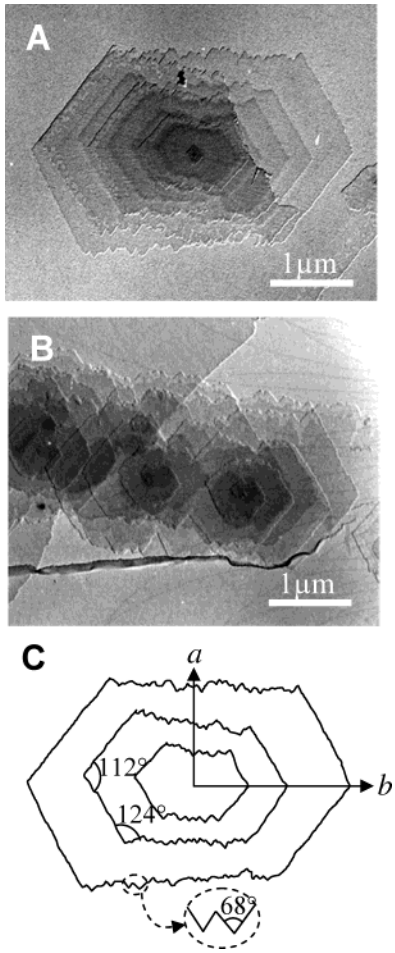

Figure 2. Transmission electron micrographs after shadowing with Pt−Pd alloy of PUDL lamellar single crystals: (A) hexagonal-shaped multilayer crystals, (B) hexagonal-shaped crystals with screw dislocations, and (C) a schematic display of hexagonal-shaped single crystals of (A).

Figure 2 shows the hexagonal-shaped multilayered single crystals without (A) and with (B) screw dislocations. Compared with the smooth faces well-defined by {110} of a lozenge-shaped crystal, the growth faces of hexagonal-shaped crystal, except {110} planes, were very rough. These rough growth faces are considered as {100} growth faces caused by the different growth speed. The angle of the jagged line was 68°, which is perfectly the same as that between {110} planes of lozenge-shaped crystal. This result indicates that the actual growth planes of {100} consist of {110} growth planes. The investigation of numerous lamellar single crystals demonstrated that screw dislocation patterns of both right- and left-handedness occur randomly as shown in Figure 2B. Until now, it was believed that the

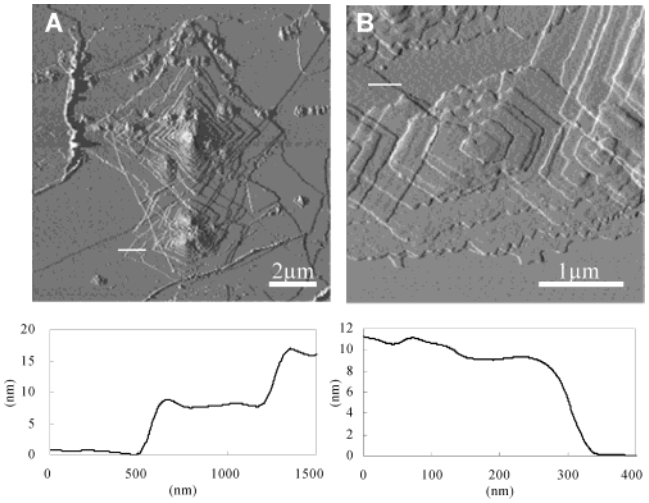

Figure 3. AFM images and line profile data of PUDL crystals: (A) lozenge-shaped and (B) hexagonal-shaped.

main chirality of molecular chain is involved in the determination of the handedness of screw dislocations in lamellar crystals. Recently, Iwata and Doi[49] and Saracovan et al.[50] concluded that the handedness of screw dislocations were not affected by the main-chain chirality based on the observation of single crystals of (*R*)- and (*S*)-poly(epichlorohydrine), (*R*)- and (*S*)-poly(propylene oxide), and P(3HV). In the case of PUDL, the molecular chain has no chirality, as is the case for poly(ethylene succinate) which has spiral growths originating from screw dislocations with both left-handed and right-handed forms.[51] A possible explanation is that the conformational variations of molecular chains might be involved in determining the handedness of screw dislocations in lamellar crystals.

AFM images of the lozenge-shaped and the hexagonal-shaped single crystals are shown in parts A and B of Figure 3, respectively. The lamellar thickness of PUDL single crystals is about 8−10 nm despite the different morphologies. Taking the length of the all-trans conformation of PUDL molecules and molecular weight into consideration, the average contour length of our PUDL chains was estimated to be 380 nm, and therefore the molecular chains of PUDL must be folded within the lamella. The crystals, which consist of stacks of lamellae, have various thicknesses: some are transparent to the electron beam, whereas others are completely opaque. Each monolamellar part at the edge of all PUDL single crystals yields a well-resolved electron diffraction diagrams. Figure 4 shows the selected-area electron diffraction diagram of the lozenge-shaped lamellar crystals. The diffraction contains 13 independent diffraction spots mirrored in the four quadrants, defined by the two orthogonal axes a^* and b^*. Along these two axes, systematic absences occur at every odd reflection. Thus, this diffraction pattern is consistent with a *p2gg* symmetry. On calibration of the electron diffraction pattern, all the electron diffraction spots can be indexed in terms of the orthogonal reciprocal lattice with the parameters $a^* = 1.346$ nm^{-1}, $b^* = 2.004$ nm^{-1}, and $\gamma^* = 90°$. A comparison of the observed and calculated *d*-spacings in the electron diffraction diagram is shown in Table 1.

X-ray Diffraction. The wide-angle X-ray diffraction pattern obtained from an oriented, sedimented mat of PUDL single crystals prepared from 1-hexanol is shown in Figure 5, and the measured diffraction spacings are

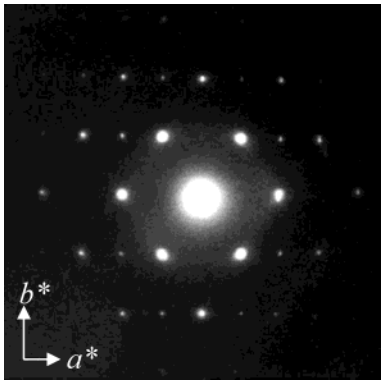

Figure 4. Selected-area (*hk*0) electron diffraction diagram of PUDL lamellar single crystal.

Table 1. Crystallographic Data for PUDL Deduced from Electron Diffraction Diagram of Single Crystals

*hk*0[a]	d_{obs} (nm)	d_{calc} (nm)	$\|F_{obs}\|^b$	$\|F_{calc}\|$
1 1 0	0.416	0.414	325.22	286.24
2 0 0	0.374	0.372	288.60	297.71
2 1 0	0.298	0.298	64.01	67.84
0 2 0	0.249	0.249	95.95	101.87
1 2 0	0.236	0.236	33.59	51.59
3 1 0	0.221	0.222	113.06	130.68
2 2 0	0.207	0.207	75.48	73.01
4 0 0	0.186	0.186	83.58	113.69
3 2 0	0.175	0.176	44.92	63.92
1 3 0	0.162	0.162	33.76	33.18
2 3 0	0.151	0.152	22.61	57.73
4 2 0	0.148	0.149	38.37	45.58
3 3 0	0.137	0.138	22.07	20.96

[a] Indexed in terms of an orthorhombic unit cell with parameters: $a = 0.743$ nm, $b = 0.499$ nm, c(fiber axis) $= 1.519$ nm. [b] $F_{obs} = (I_{obs})^{1/2}$, $\sum I_{obs} = \sum I_{calc}$.

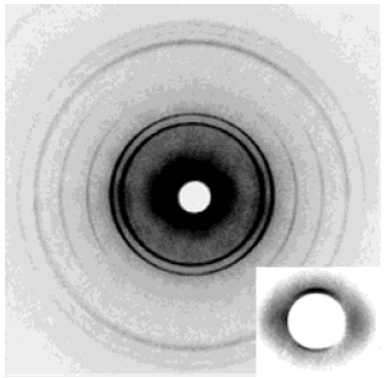

Figure 5. Wide-angle X-ray diffraction pattern from oriented, sedimented single-crystal mats of PUDL; incident beam parallel to mat surface and mat normal vertical. Low-angle diffraction pattern of (001) is shown in the enlarged figure of the lower right inset.

Table 2. Crystallographic Data for PUDL Deduced from X-ray Diffraction Pattern of Sedimented Mat of Lamellar Single Crystals

hkl[a]	d_{obs} (nm)	d_{calc} (nm)	*hkl*[a]	d_{obs} (nm)	d_{calc} (nm)
1 1 0	0.415	0.414	0 0 1	1.506	1.519
2 0 0	0.366	0.372	3 1 4	0.190	0.192
2 1 0	0.282	0.298	3 1 5	0.180	0.179
3 1 0	0.224	0.222	3 1 6	0.171	0.167
4 0 0	0.189	0.186	3 1 8	0.147	0.144

[a] Indexed in terms of an orthorhombic unit cell with parameters: $a = 0.743$ nm, $b = 0.499$ nm, c(fiber axis) $= 1.519$ nm.

listed in Table 2. Apart from some specific overlaying diffraction features, the diffraction signals index on an orthorhombic unit cell with the parameters $a = 0.743$

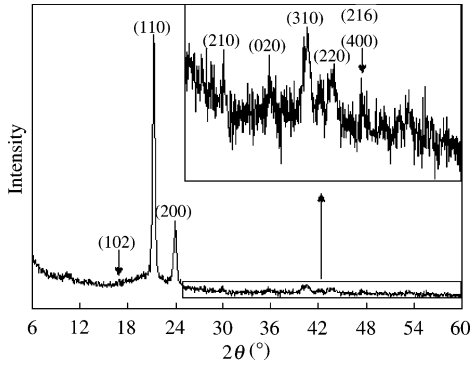

Figure 6. X-ray diffraction pattern of PUDL annealed solvent-cast film.

Table 3. Crystallographic Data for PUDL Deduced from the X-ray Diagram of Annealed Solvent-Cast Film

hkl[a]	d_{obs} (nm)	d_{calc} (nm)	$\|F_{obs}\|$	$\|F_{calc}\|$
1 0 2	0.520	0.531	34.64	33.26
0 1 1	0.479	0.474	38.73	41.29
1 1 0	0.415	0.414	325.42	315.72
2 0 0	0.371	0.372	220.45	209.52
2 1 0	0.299	0.298	70.71	61.72
2 1 2	0.279	0.277	30.00	32.36
0 2 0	0.251	0.249	34.64	45.12
1 0 6	0.238	0.239	31.62	40.36
1 2 0		0.236		29.71
0 1 6	0.226	0.225	30.00	45.72
3 1 0	0.223	0.222	41.23	79.32
2 0 6	0.210	0.209	31.62	29.60
2 2 0	0.207	0.207	31.62	42.99
2 1 6	0.191	0.193	31.62	52.58
4 0 0		0.186		36.67
3 0 6	0.177	0.177	30.00	37.47
1 2 6	0.173	0.173	20.00	39.77

[a] Indexed in terms of an orthorhombic unit cell with parameters: $a = 0.743$ nm, $b = 0.499$ nm, c(fiber axis) $= 1.519$ nm.

$\pm$ 0.001 nm, $b = 0.499 \pm 0.001$ nm, and c (chain axis) $=$ 1.519 ± 0.003 nm. The a and b values match those determined from the electron diffraction pattern and confirm that the electron diffraction diagram represents the $hk0$ reciprocal lattice; that is, the straight-stem segments are orthogonal to the lamellar surface.

Figure 6 shows the PUDL X-ray diffraction pattern of annealed solvent-cast films. It is characterized by two strong reflections at 2θ equal to 21.40° and 23.90°, corresponding to $d = 0.415$ and 0.371 nm indexed by (110) and (200), respectively. There is a close similarity between the X-ray diffraction pattern of PUDL and those of PPL,[27] PVL,[32] and PCL.[33] They are associated with the lateral packing distances between the polymer chains. A unit cell with the same a and b dimensions as PPL[27] and PVL,[32] but with a longer c-axis value obtained from the small-angle reflection, was selected as the starting cell. The observed d-spacings in the X-ray diffraction pattern are listed in Table 3.

Determination of Unit Cell. The unit cell parameters were determined through the electron diffraction pattern (Figure 4) and the X-ray diffraction diagram of a single-crystal mat (Figure 5) and the X-ray diffraction pattern of annealed solvent-cast films (Figure 6). The X-ray diffraction profile has a lower resolution than the electron diffraction diagram that displays diffraction spots down to 0.137 nm spacing as opposed to only 0.186 nm for the X-ray diffraction. PUDL crystallized as an orthorhombic form with lattice constants of $a = 0.743$ $\pm$ 0.001 nm, $b = 0.499 \pm 0.001$ nm, and c(chain axis) $=$ 1.519 ± 0.003 nm.

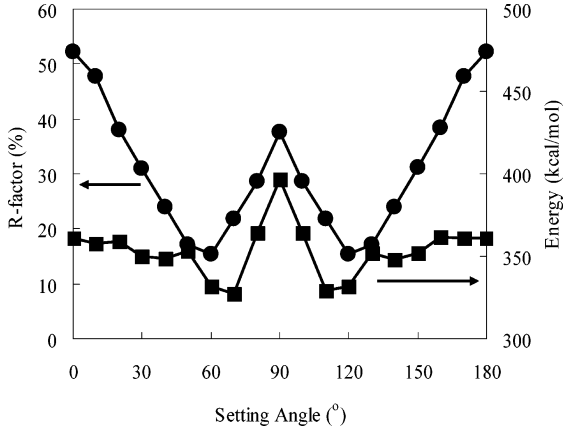

Figure 7. Reliability factor (R-factor, ●) and energy (■) as a function of the setting angles with respect to the a axis. The observed intensities of the electron diffraction diagram as listed in Table 1 were used to calculate the R-factor.

Further information was deduced from the density measurements of crystalline PUDL. An observed value ($\rho_{obs.}$) of 1.045 g/cm^3 is found. This value closely matches the theoretical value ($\rho_{calc.}$) of 1.085 g/cm^3, deduced from the cell parameters and assuming that two chains pass through the unit cell. PUDL has chain polarity, and so a minimum of two chain segments per unit cell is also a necessary condition for chain-folded crystals.

The refined a and b lattice parameters of PUDL ($a =$ 0.743 nm and $b = 0.499$ nm) are very close to those of PVL ($a = 0.502$ nm and $b = 0.747$ nm)[32] and PPDL (a $= 0.749$ nm and $b = 0.503$ nm)[37] and only slightly larger than those of PPL ($a = 0.700$ nm and $b = 0.490$ nm),[27] indicating that the lateral cell expansion due to the C═O groups does not depend on the number of methylene units in the chain. On the other hand, the c parameters increased with an increase in the number of methylene units in the chain because of molecular chain having planar zigzag conformation. The planar zigzag conformation of the PUDL chain is reasonable because its chain extension agrees with the length of the unit cell c-axis. Our assumption agrees with previous results,[27,28,32,37] suggesting that linear aliphatic polyesters with even or odd number of methylene units in the backbone adopt all-trans or close to all-trans conformation.

Chain-Packing Structure. The measured fiber repeat distance of 1.519 ± 0.003 nm matched the value found from the modeling of an all-trans, 1-fold helical chain conformation. The refinement of the structure was undertaken in stages and involved detailed stereochemical packing calculations, coupled with matching of the intensity values, from both electron diffraction and X-ray diffraction patterns. In the first instance, the chains were kept in an all-trans conformation, and the initial setting angles were determined from the intensity distribution given by the electron diffraction $hk0$ data (Table 1).

Packing of polymer chains in the crystal including setting angle orientations and the relative shift of molecules in the unit cell are often studied taking into account both experimental diffraction data and energy calculation. A reliability factor (R-factor) study was carried out in order to determine the most favorable setting angle. For this purpose, the setting angle, θ, with respect to the a axis, was varied from 0° to 180° in steps of 10°, and the R-factor and energy were evaluated. Figure 7 shows the R-factor against electron diffraction

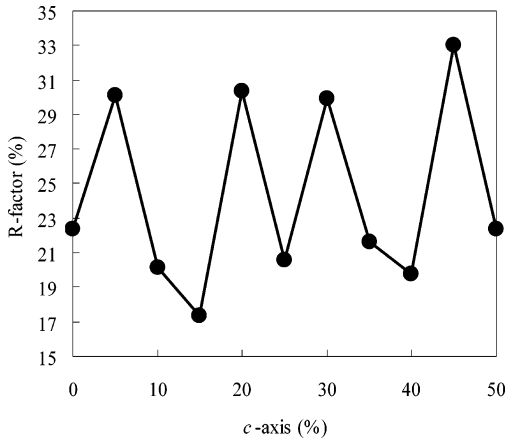

Figure 8. Reliability factor (*R*-factor) as a function of the changed position along the *c* axis. The observed intensities of the X-ray diffraction as listed in Table 3 were used to calculate the *R*-factor.

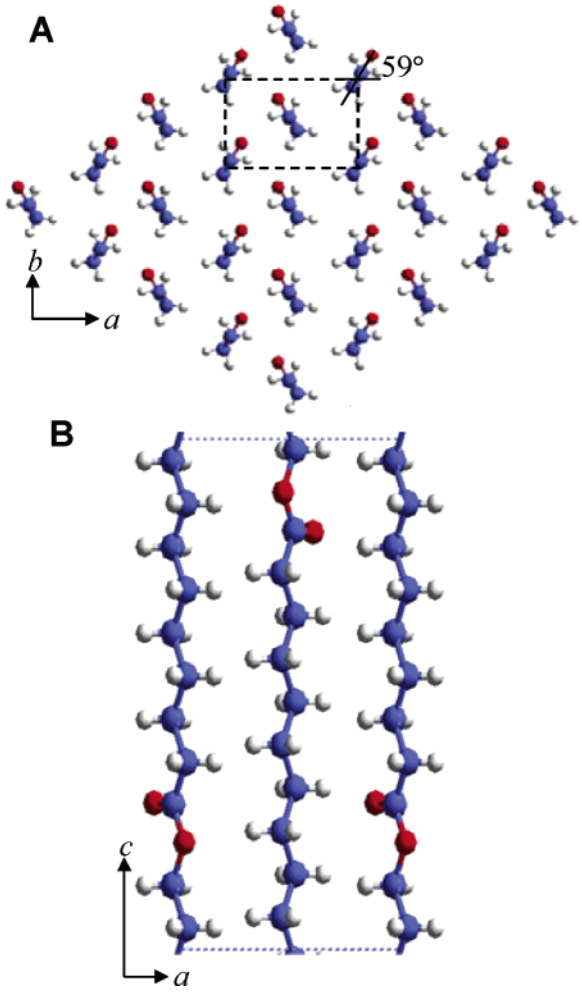

Figure 9. (A) Projection of the PUDL structure in the *ab* plane. (B) Projection of the PUDL structure in the *ac* plane.

data and energy as a function of the setting angle θ with respect to the *a* axis. The most favorable arrangement corresponded to $\theta = 60°$ and 120° as for the *R*-factor. Accordingly, the *R*-factor and setting angle map was recomputed using finer grid steps, 1°, from 50° to 70°. The results showed that the most favorable arrangement was 59° with respect to the *a* axis, as shown in Figure 9A. The rotation angles between the plane of the polymer chain and the *a* axis are 51.5° for PPL,[27] 58° for PVL,[32] and 61° for P(4HB).[28] Recently, the crystal structure of PPDL[37] was determined by Gazzano et al., and they reported that the backbone conformation is all-trans and the setting angle, with respect to the *a* axis is 48°. The stable position of molecular chains with the all-trans conformation around the molecular axis seems to be almost the same. A comparison of the observed and calculated structure factors is given in Table 1, and as a test for goodness of fit, the calculated reliable index *R* was 0.152.

Table 4. Bond Lengths, Bond Angles, and Torsion Angles of the PUDL Molecular Chain

Bond Lengths (nm)			
O_1-C_1	0.135	$C_{11}-O_1$	0.148
$C_1=O_2$	0.123	C_n-C_{n+1}	0.154
C_1-C_2	0.151	($n = 2-10$)	
Bond Angles (deg)			
$O_1-C_1=O_2$	125.0	$C_{10}-C_{11}-O_1$	115.0
$O_1-C_1-C_2$	114.0	$C_{11}-O_1-C_1$	116.0
$O_2=C_1-C_2$	121.0	$C_n-C_{n+1}-C_{n+2}$	112.5
$C_1-C_2-C_3$	113.0	($n = 2-9$)	
Torsion Angles (deg)			
all of torsion angle is 180°			

The translation along the molecular axis was carried out against X-ray diffraction intensity data. The shift parameter along the molecular axis was changed from 0 to 0.5*c* ($c = 1.519$ nm) at the rate of 0.05*c* (as shown in Figure 8). Since the unit cell has 2-fold screw symmetry along the *a* and *b* and two antiparallel chains exist in it, this translation of up to 0.5*c* covers all translation position. The optimized shift value along the molecular axis was 0.15*c*. A comparison of the observed and calculated structure factors is given in Table 3, and as a test for goodness of fit, the calculated reliable index *R* was 0.173 (as shown in Figure 8).

Perhaps it is worth mentioning at this stage that models have been proposed for the aliphatic polyester PCL[33] and P(4HB)[28] in which the ester group twists slightly out of the all-trans conformation, although in a separate analysis an all-trans conformation was favored. For PUDL, no particular improvement in goodness of fit was obtained by the introduction of perturbations into the all-trans backbone. Certainly, the measured *c* repeat of PUDL matches the all-trans conformation rather well. The stereochemical parameters of the straight stem are given in Table 4.

A final model was obtained which yielded $R = 0.173$ with X-ray diffraction data and $R = 0.152$ with electron diffraction data. The lists of observed and calculated structure factors with the final model are presented in Tables 2 and 3 for electron and X-ray diffraction data, respectively. The list of the fractional coordinates is presented in Table 5, and the packing of the chain in the crystal is shown in projection in Figure 9.

The repetitive segment in the chain-folded lamella can, therefore, be defined as follows: from the lamellar core center of a (unit cell) corner chain through a fold, through an antiparallel center chain, through a second fold, and back to the center of another corner chain. We know a priori that chain-folding must occur within the diagonal {110} planes.

Conclusion

The crystal structure of poly(11-undecalactone) (PUDL) has been determined by the analysis of X-ray and electron diffraction patterns of annealed solvent-cast film and single-crystal specimens. The unit cell of PUDL

Table 5. Fractional Atomic Coordinates of PUDL

atom	*x*	*y*	*z*
O_1	+0.0268	−0.0668	+0.2092
O_2	−0.1099	+0.2693	+0.2870
C_1	−0.0236	+0.0591	+0.2839
C_2	+0.0334	−0.0829	+0.3667
C_3	−0.0258	+0.0646	+0.4511
C_4	+0.0333	−0.0827	+0.5354
C_5	−0.0259	+0.0648	+0.6198
C_6	+0.0332	−0.0825	+0.7041
C_7	−0.0260	+0.0650	+0.7885
C_8	+0.0331	−0.0823	+0.8728
C_9	−0.0261	+0.0652	+0.9572
C_{10}	+0.0330	−0.0821	+1.0415
C_{11}	−0.0262	+0.0654	+1.1259

is orthorhombic with the unit cell parameters $a = 0.743 \pm 0.001$ nm, $b = 0.499 \pm 0.001$ nm, and c(chain axis) $= 1.519 \pm 0.003$ nm. Lamellar single crystals grown in 1-hexanol were lozenge- and hexagonal-shaped. The {110} planes were the main growth planes of single crystals, and the average direction of chain-folding was parallel to these growth planes. The density supports a model containing two antiparallel chain segments, which have all-trans conformation, in the unit cell. The refinement of the structure was undertaken in stages and involved detailed stereochemical packing calculations, coupled with matching of the intensity values, from both electron diffraction and X-ray diffraction patterns by computer simulation program, Cerius[2]. The setting angles, with respect to the *a* axis, were ±59° for the corner and center chains, respectively. A final model yielded $R = 0.173$ with X-ray diffraction data and $R = 0.152$ with electron diffraction data.

Acknowledgment. E.K. was a recipient of a two-year fellowship of Joint Graduate School Program of RIKEN Institute, Japan. This work has been supported by a grant for Ecomolecular Science Research to RIKEN Institute and a Grant-in-Aid for Young Scientists (A) No. 15685009 (2003) from the Ministry of Education, Culture, Sports, Science and Technology, Japan (to T.I.). C.-S.H. thanks the National Research Laboratory Program. We thank Dr. K. Sudesh for the English correction of our manuscript.

References and Notes

(1) Kobayashi, S.; Shoda, S.; Uyama, H. In *Catalysis in Precision Polymerization*; Kobayashi,, S., Ed.; John Wiley & Sons: Chichester, 1997; Chapter 8.
(2) Kobayashi, S.; Shoda, S.; Uyama, H. *Adv. Polym. Sci.* **1995**, *121*, 1.
(3) Ritter, H. *Trends Polym. Sci.* **1993**, *1*, 171.
(4) Kobayashi, S.; Uyama, H. *ACS Symp. Ser.* **1998**, *684*, 58.
(5) Wallace, J. S.; Morrow, C. J. *J. Polym. Sci., Polym. Chem. Ed.* **1989**, *27*, 2553.
(6) Namekawa, S.; Uyama, H.; Kobayashi, S. *Polym. J.* **1996**, *28*, 730.
(7) Matsumura, S.; Beppu, H.; Nakamura, K.; Osanai, S.; Toshima, K. *Chem. Lett.* **1996**, 795.
(8) Svirkin, Y. Y.; Xu, J.; Gross, R. A.; Kaplan, D. L.; Swift, G. *Macromolecules* **1996**, *29*, 4591.
(9) Nobes, G. A. R.; Kazlauskas, R. J.; Marchessault, R. H. *Macromolecules* **1996**, *29*, 4829.
(10) Xie, W.; Li, J.; Chen, D.; Wang, P. G. *Macromolecules* **1997**, *30*, 6997.
(11) Knani, D.; Gutman, A. L.; Kohn, D. H. *J. Polym. Sci., Polym. Chem. Ed.* **1993**, *31*, 1221.
(12) Uyama, H.; Kobayashi, S. *Chem. Lett.* **1993**, 1149.
(13) MacDonald, R. T.; Pulapura, S. K.; Svirkin, Y. Y.; Gross, R. A.; Kaplan, D. L.; Akkara, J. A.; Swift, G.; Wolk, S. *Macromolecules* **1995**, *28*, 73.
(14) Uyama, H.; Takeya, K.; Kobayashi, S. *Proc. Jpn. Acad.* **1993**, *69B*, 203.
(15) Uyama, H.; Takeya, K.; Kobayashi, S. *Bull. Chem. Soc. Jpn.* **1995**, *68*, 56.
(16) Uyama, H.; Takeya, K.; Hoshi, N.; Kobayashi, S. *Macromolecules* **1995**, *28*, 7046.
(17) Uyama, H.; Kikuchi, H.; Takeya, K.; Kobayashi, S. *Acta Polym.* **1996**, *47*, 357.
(18) Bisht, K. S.; Henderson, L. A.; Gross, R. A.; Kaplan, D. L.; Swift, G. *Macromolecules* **1997**, *30*, 2705.
(19) Namekawa, S.; Uyama, H.; Kobayashi, S. *Proc. Jpn. Acad.* **1998**, *74* (Ser. B), 65.
(20) Matsumura, S.; Mabuchi, K.; Toshima, K. *Macromol. Rapid Commun.* **1997**, *18*, 477.
(21) Matsumura, S.; Tsukuda, K.; Toshima, K. *Macromolecules* **1997**, *30*, 3122.
(22) Kobayashi, S.; Kikuchi, H.; Uyama, H. *Macromol. Rapid Commun.* **1997**, *18*, 575.
(23) Bisht, K. S.; Svirkin, Y. Y.; Henderson, L. A.; Gross, R. A.; Kaplan, D. L.; Swift, G. *Macromolecules* **1997**, *30*, 7735.
(24) Uyama, H.; Namekawa, S. *Polym. J.* **1997**, *29*, 299.
(25) Wasai, T.; Saegusa, T.; Furukawa, *J. Chem. Soc. Jpn., Ind. Chem. Sect.* **1964**, *67*, 601.
(26) Suehiro, K.; Chatani, Y.; Tadokoro, H. *Polym. J.* **1974**, *7*, 352.
(27) Furuhashi, Y.; Iwata, T.; Sikorski, P.; Atkins, E.; Doi, Y. *Macromolecules* **2000**, *33*, 9432.
(28) Su, F.; Iwata, T.; Tanaka, F.; Doi, Y. *Macromolecules* **2003**, *36*, 6401.
(29) Mitomo, H.; Kobayashi, S.; Morishita, N.; Doi, Y. *Polym. Prepr., Jpn.* **1995**, *44*, 3156.
(30) Kobayashi, S.; Kogure, K.; Mitomo, H.; Doi, Y. *Polym. Prepr., Jpn.* **1998**, *47*, 968.
(31) Pazur, R. J.; Raymond, S.; Hocking, P. J.; Marchessault, R. H. *Polymer* **1998**, *39*, 3065.
(32) Nakamura, K.; Yoshie, N.; Sakurai, M.; Inoue, Y. *Polymer* **1994**, *35*, 193.
(33) Su, F.; Iwata, T.; Sudesh, K.; Doi, Y. *Polymer* **2001**, *42*, 8915.
(34) Furuhashi, Y.; Sikorski, P.; Atkins, E.; Iwata, T.; Doi, Y. *J. Polym. Sci., Part B: Polym. Phys.* **2001**, *39*, 2622.
(35) Bittiger, H.; Marchessault, R. H. *Acta Crystallogr.* **1970**, *B26*, 1923.
(36) Chatani, Y.; Okita, Y.; Tadokoro, H.; Yamashita, Y. *Polym. J.* **1970**, *1*, 555.
(37) Hu, H.; Dorset, D. L. *Macromolecules* **1990**, *23*, 4604.
(38) Dorset, D. L. *Proc. Natl. Acad. Sci. U.S.A.* **1991**, *88*, 5499.
(39) Dorset, D. L. *Polymer* **1997**, *38*, 247.
(40) Iwata, T.; Doi, Y. *Polym. Int.* **2002**, *51*, 852.
(41) Gazzano, M.; Malta, V.; Focarete, M. L.; Scandola, M. *J. Polym. Sci., Part B: Polym. Phys.* **2003**, *41*, 1009.
(42) Pazur, R. J.; Hocking, P. J.; Raymond, S.; Marchessault, R. H. *Macromolecules* **1998**, *31*, 6585.
(43) Bruckner, S.; Meille, S. V.; Malpezzi, L.; Cesàro, A.; Navarini, L.; Tombolini, R. *Macromolecules* **1988**, *21*, 967.
(44) Keller, A.; Willmouth *J. Polym. Sci., Part A-2* **1970**, *8*, 1443.
(45) Dorset, D. L. *Acta Crystallogr.* **1976**, *A32*, 207.
(46) Reneker, D. H.; Geil, P. H. *J. Appl. Phys.* **1960**, *31*, 1916.
(47) Geil, P. H. *Polymer* **1963**, *4*, 404.
(48) Iwata, T.; Doi, Y. *Macromolecules* **2000**, *33*, 5559.
(49) Iwata, T.; Doi, Y. *Macromolecules* **2000**, *33*, 5559.
(50) Saracovan, I.; Cox, J. K.; Revol, J. F.; Manley, R. St. J.; Brown, G. R. *Macromolecules* **1999**, *32*, 717.
(51) Iwata, T.; Doi, Y.; Isono, K.; Yoshida, Y. *Macromolecules* **2001**, *34*, 7343.

MA0492871